

ADC Diversity for Software Defined Radios

Ying Chen, André Pollok, David Haley and Linda M. Davis

Institute for Telecommunications Research

University of South Australia

Adelaide, Australia

{Ying.Chen, Andre.Pollok, David.Haley, Linda.Davis}@unisa.edu.au

Abstract—Rapidly evolving digital processing architectures are a key technology enabler for software defined radio (SDR). The flexibility of SDR is dependent upon a high speed front end that can provide large dynamic range and noise resilience in transferring from the analog to digital domain. The analog to digital converter (ADC) is a key component within the front end, and recent architectures have been proposed that make use of parallel ADCs to improve signal-to-noise ratio (SNR) or increase dynamic range.

Motivated by the SNR gains offered by multi-antenna receive diversity schemes, in this paper we show how similar techniques can be applied to the use of parallel ADC architectures. We provide a generalized model for the parallel ADC front end architecture, and show how it can represent existing techniques from the literature. The architecture is then used to develop new methods for low complexity ADC output combining. We propose a novel ADC combining scheme that is able to simultaneously improve SNR and dynamic range by reducing the impact of both quantization noise and saturation.

I. INTRODUCTION

The software defined radio (SDR) concept offers physical layer flexibility and real time adaptability [1]. In order to realize these benefits, SDR requires advancement in technology enabling subsystems. The SDR goal of digital domain processing motivates a flexible front end interface, making the analog to digital converter (ADC) a key component [2]. The flexibility and reprogrammability of SDR makes it attractive for mobile and remote deployment applications such as satellite payloads and sensor networks. These applications often carry tight size, weight and power constraints, necessitating low powered analog components and low complexity digital front end processing. In order to offer robust wideband support the ADC should provide high dynamic range, while also being resilient to noise. The front end typically also includes an automatic gain control (AGC) stage, which controls the ADC input level with the goal of maximising ADC output signal quality. The AGC targets an ADC input *operating point* that reduces the effective quantization noise by maximizing input dynamic range without overdriving the ADC into saturation [3].

An overview of the state-of-the art in ADC technology is presented in [2]. The author identifies a gap between current techniques and the needs of SDR. Limiting factors include finite sample rate and dynamic range, and the presence of

noise. In addition to quantization and clipping (saturation) noise, other sources include sample clock jitter, imperfections in sample-and-hold circuitry (aperture jitter) and thermal noise.

Several approaches have been proposed that employ parallel ADCs to improve performance. The *signal averaging* architecture proposed in [4] and [5] reduces the impact of uncorrelated noise generated by the ADC components. However the approach does not improve resilience to quantization and clipping noise. It is noted in [5] that dithering may reduce correlation of quantization noise between ADCs. An alternate use of parallel ADCs is proposed in [6] which reduces the effect of clipping noise in order to increase dynamic range. The architecture includes two parallel ADCs, with an attenuator placed at the input to one of the devices. If the direct path ADC begins to clip, the circuit switches to the ADC with the attenuated input, hence performing *selection combining*. However, the method does not fully explore the potential for the digital signal processing to also reduce the effective quantization noise within the extended dynamic range. Time interleaving of parallel ADCs has also been proposed as a means to increase sample rate [7].

Motivated by the signal-to-noise ratio (SNR) gains achievable using multi-antenna receive diversity [8], in this paper we consider how similar techniques can be applied to the use of parallel ADC architectures. A general model is described for a single antenna receiver which includes parallel ADC branches that feed digital signal processing. The paper explores signal processing methods to combine ADC outputs with dual goals of increasing dynamic range and SNR. We observe an analogy between ADC signal averaging [4] and equal gain combining for multi-antenna receivers. Similarly, ADC selection combining [6] is analogous to multi-antenna selection diversity. Maximal ratio combining is an optimal SNR achieving multi-antenna receive technique. The method weights each receive branch independently in proportion to its SNR, and then combines branches [8]. This approach motivates us to consider weighted combining of ADC branches, in contrast to signal averaging or selection.

In Section II of this paper we introduce expressions for ADC quantization and clipping. The conventional single ADC system with automatic gain control is introduced and analyzed in Section III. We propose a generalized parallel ADC architecture and modeling framework in Section IV. The framework is

This research was supported under the Australian Government's Australian Space Research Program.

able to represent existing techniques such as signal averaging and selection combining. Using this framework, in Section V we then develop novel methods for ADC output combining. We propose a new *gain weighted combining* technique that individually weights the contribution of each ADC branch to improve SNR. A novel *hybrid combining* approach is then proposed that is able to reduce the impact of both clipping and quantization noise, and thus increase dynamic range and SNR. The simulation performance of the new ADC combining techniques is compared to existing approaches in Section VI. We provide concluding remarks in Section VII.

II. QUANTIZATION AND CLIPPING

Let Δ be the quantization step and let b denote the number of *effective* bits of the ADC, i.e. b does not include the sign bit and hence, the ADC has $2^b - 1$ quantization levels symmetrically placed on either side of the zero level, in addition to the zero level (mid-tread). The most negative and positive input values that are not clipped by saturation (but may be rounded) by the ADC are given by $\pm A$, where $A = (2^b - 1 + \frac{1}{2})\Delta$. Assuming an ideal ADC without nonlinearities, thermal noise or spurious components, an input signal y in the range $-A < y < A$ gives rise to

$$\hat{y} = m\Delta, \quad (1)$$

$$m = \left\lfloor \frac{y}{\Delta} \right\rfloor \quad (2)$$

at the output of the ADC, where $\lfloor \cdot \rfloor$ rounds the argument to the nearest integer. Note that $m \in \{0, \pm 1, \dots, \pm(2^b - 1)\}$.

In this paper we consider only uniform quantization. An overview of non-uniform quantization techniques is provided in [2].

A. Quantization Errors

The signal distortion caused by the rounding operation in (2) is referred to as *quantization error*. Let e_q denote the quantization error

$$e_q(y) = y - \hat{y} = y - m\Delta. \quad (3)$$

Assuming that the input signal can be modeled as a random variable with probability density function (pdf) $f(y)$, the variance of the quantization error, σ_q^2 , can be computed from [9]

$$\sigma_q^2(y) = \sum_{m=-2^{b-1}+1}^{2^{b-1}-1} \int_{(m-\frac{1}{2})\Delta}^{(m+\frac{1}{2})\Delta} f(y) e_q^2(y) dy. \quad (4)$$

If y is uniformly distributed over the entire dynamic range of the ADC, its pdf is given by $f(y) = \frac{1}{2(2^b-1)\Delta}$ and (4) will result in the well-known expression $\sigma_q^2(y) = \frac{\Delta^2}{12}$ [9].

B. Clipping Errors

A second type of signal distortion arises from the fact that the dynamic range A of an ADC is finite. An input signal exceeding this finite range, i.e. $y > A$, will overdrive the ADC

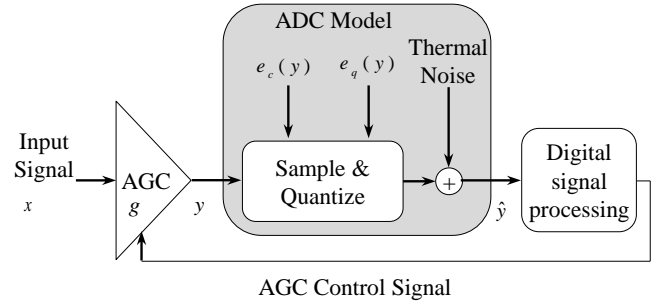


Fig. 1. Block diagram for conventional AGC and ADC.

into saturation. This type of distortion is referred to as *clipping error* and we define it as

$$e_c(y) = \begin{cases} y - A, & y > +A \\ y + A, & y < -A \\ 0, & \text{otherwise.} \end{cases} \quad (5)$$

Assuming that the distribution of y is symmetric about zero, the variance of the clipping noise can be obtained as

$$\sigma_c^2(y) = 2 \int_A^\infty f(y) e_c^2(y) dy \quad (6)$$

To simplify the analysis, at this point we ignore thermal noise and any other distortions of the radio frequency (RF) chain and only consider the signal to quantization and clipping noise ratio

$$\text{SNR}_{c,q} = \frac{P(y)}{\sigma_c^2(y) + \sigma_q^2(y)}, \quad (7)$$

where $P(y)$ denotes the average power of y .

III. CONVENTIONAL AGC AND ADC

Quantization error and clipping error introduced by the ADC will limit the available signal to noise ratio (SNR), as can be seen in equation (7). To minimize the impacts of these errors, an AGC is typically used in the receiver to adjust the ADC input signal power [10]. As shown in Fig. 1, the input signal x is fed to the AGC with gain g to generate an output signal $y = gx$. This signal is then sampled and quantized by the ADC to yield a digital signal \hat{y} . This digitized signal will be used in the digital signal processing part of the receiver to reconstruct the source data. During the analog to digital conversion process, quantization errors and clipping errors are introduced, as well as additive thermal noise generated by the electronic components of the ADC. The thermal noise is practically modeled as a fixed noise floor in the ADC [5] and is not related to the input signal. In contrast, equations (4) and (6) show that the quantization and clipping errors are related to the distribution and power of the input signal.

In what follows, we analyze the relationship between the AGC gain g and ADC performance, treating the ADC as an ideal quantizer. As reviewed in Section II, the clipping error variance σ_c^2 and the quantization error variance σ_q^2 are related to the probability density function of the input signal. We

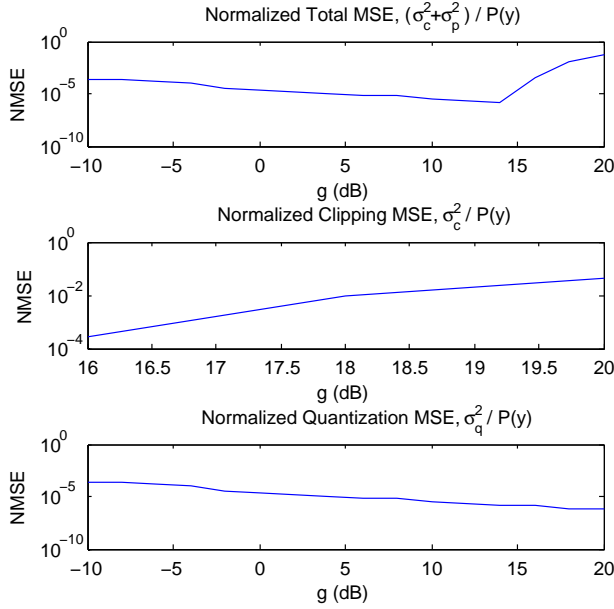


Fig. 2. Mean square noise power for 10-bit ADC, uniformly distributed input.

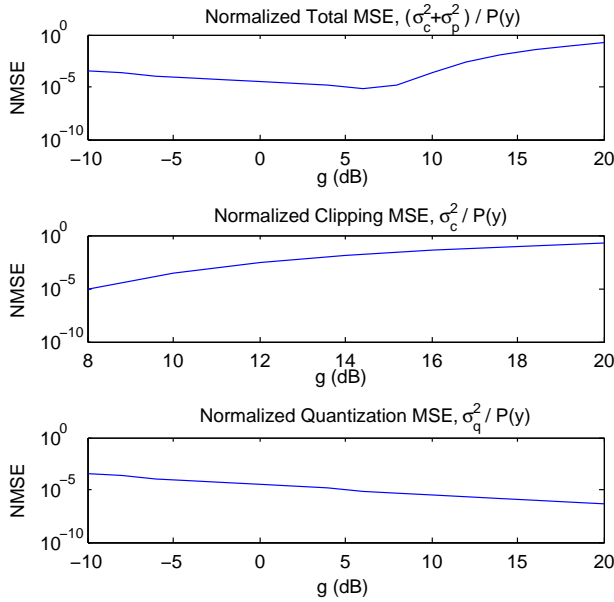


Fig. 3. Mean square noise power for 10-bit ADC, Gaussian distributed input.

numerically test the normalized mean square error (MSE) as a measure of the normalized variance between the ADC inputs and outputs and its components for a 10-bit ADC. Results are provided for a uniformly distributed input coming from an 8-times oversampled BPSK modulated signal, and for a Gaussian distributed input coming from a multicarrier signal with 512 subcarriers. Figs. 2 and 3 show the relationship between g and the ADC performance. The figures show the impact of clipping and quantization errors, along with the combined impact, normalizing the total MSE to the input signal power. We note that the combined normalized MSE is the inverse of the signal to quantization and clipping noise

ratio in equation (7).

The basic relationship between the AGC gain g and the normalized MSEs is similar for the different inputs of Figs. 2 and 3. When g is small, the total error is dominated by the quantization error. The clipping error is zero for the uniform distributed input and small for the Gaussian distributed input. As g increases, the impact of clipping error increases and eventually dominates the total error. From these plots the value of g that provides the smallest total error is 14 dB for the uniform distributed signal and 6 dB for the Gaussian distributed signal. The difference in these values is due to the fact that a Gaussian distributed signal has a large peak to average power ratio whereas the uniformly distributed signal has a small peak to average power ratio [11]. The plots illustrate that we cannot simultaneously improve the resilience to quantization error and clipping error by varying the AGC gain. In order to address this issue we propose the use of parallel ADC branches. In the next section we will discuss the architecture in detail.

IV. PARALLEL ADC ARCHITECTURE

The results from Section III show that conventional AGC can only increase dynamic range at the expense of decreasing the achievable signal to quantization noise ratio of a given ADC. In [6], a selection diversity scheme is proposed that uses dual ADC branches. The input to one branch is attenuated, extending its relative saturation point and thus increase dynamic range. Signal averaging [4] provides an alternate parallel ADC architecture which aims to improve SNR by reducing the impact of uncorrelated component noise.

In this section we generalize the parallel ADC architecture using the dual branch example shown in Fig. 4. As was the case for the single branch ADC system, the input signal x is fed to the AGC with gain g_1 to generate an output signal $y_1 = g_1 x$ on the first branch. The AGC output also feeds a second branch via a signal splitter. This branch includes a component with gain η , i.e. an amplifier or attenuator, to generate $y_2 = \eta g_1 x = g_2 x$. The signals on branch one and two are then connected to independent ADCs, both of which can be modeled as the ADC in Fig. 1. We assume that these ADCs share a common clock and hence synchronized. ADC outputs are fed to the digital signal processing stage, where a combiner is applied to the digitized signals \hat{y}_1 and \hat{y}_2 . In the next section we show that a carefully designed combiner can achieve a simultaneous improvement of the ratios of signal to quantization error and clipping error.

The architecture shown in Fig. 4 provides a generalized framework for consideration of existing ADC diversity methods and the development of new techniques. Signal averaging [4] can be considered as the special case when $\eta = 1$. Selection combining [6] can be viewed as the special case when $\eta < 1$.

V. ADC DIVERSITY COMBINING

Ultimately, we are interested in finding the most accurate quantized approximation of the continuous input signal x . In

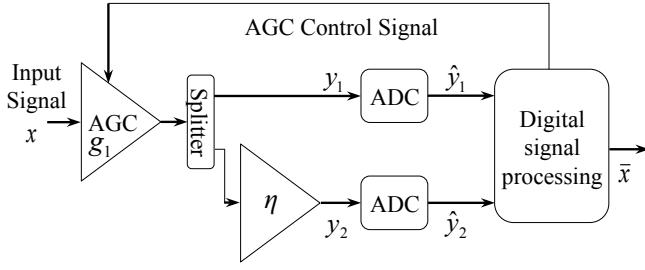


Fig. 4. Generalized parallel ADC architecture.

In this section, we discuss various approaches of combining the two output signals \hat{y}_1 and \hat{y}_2 of the parallel ADC architecture described in Section IV. Given that these signals were produced by separate ADCs, they are different observations of the same input signal and hence, provide some level of diversity. Similar to diversity combining in multi-antenna communications, the aim of ADC diversity combining is to increase the output SNR. In our case, increasing the SNR corresponds to reducing the effective levels of quantization and clipping noise relative to the signal power in the output. In other words, we would like to leverage the diversity such that the combined signal, denoted as \bar{x} , more accurately approximates x than $\hat{x}_1 = \hat{y}_1/g_1$ or $\hat{x}_2 = \hat{y}_2/g_2$ individually.

Several of the schemes that we will discuss rely on the fact that the input signals of the two ADCs are scaled versions of each other. Specifically, we assume $\eta < 1$ such that y_2 is an attenuated version of y_1 . Consequently, the ADC operating on the attenuated signal will introduce larger quantization errors relative to the signal power $P(y_2)$, but is less likely to clip the input signal (see Figs. 2 and 3).

A. Selection Diversity

Selection diversity is attractive due to its simplicity. Rather than combining \hat{y}_1 and \hat{y}_2 , the output signal that suffers the least from ADC distortions is selected. Always selecting the best branch guarantees a performance at least as good as that of a single ADC. A *selection combining* architecture with two parallel ADCs was proposed in [6], targeting an increased dynamic range. As soon as the input signal starts to overdrive the first ADC, the architecture switches to the output of the second ADC, which operates on an passively attenuated input signal and is thus less prone to clipping errors. The architecture [6] is captured by our general framework from Section IV when setting $\eta < 1$ (i.e. attenuation) and computing the combined output signal as

$$\bar{x}_{\text{sel}} = \begin{cases} \frac{\hat{y}_1}{g_1} & g_1 x \leq A \\ \frac{\hat{y}_2}{g_2} & g_1 x > A. \end{cases} \quad (8)$$

Whilst diversity combining can extend the dynamic range, it does not exploit the full potential of digital signal processing in the sense that it only selects one of the signals rather than

combining them. In particular, the selected signal has the same SQNR as that of the corresponding ADC.

B. Gain Weighted Combining

In this section, we propose a novel ADC diversity combining technique which takes advantage of the fact that both ADC output signals contain useful information about the input signal. We refer to our approach as *gain weighted combining* (GWC) and it reconstructs the input signal x as

$$\bar{x}_{\text{gwc}} = \frac{g_1 \hat{y}_1 + g_2 \hat{y}_2}{g_1^2 + g_2^2}. \quad (9)$$

Readers familiar with the multi-antenna literature will notice the similarity of (9) and maximal ratio combining. In fact, if \hat{y}_1 and \hat{y}_2 were subject to uncorrelated noise of equal variance, GWC would be equivalent to maximal ratio combining. In practice, however, we do not have this equivalence as the quantization noise of the two ADC branches is correlated. The degree of correlation is determined by η . Under the assumption that neither of the ADCs saturates, it can be shown that certain choices of η lead to negative quantization noise correlation. This negative correlation leads to an SQNR improvement in the output \bar{x}_{gwc} . Our simulation results in Section VI demonstrate that GWC with $\eta = 1/2$ provides an SNR gain of approximately 2 dB over a single ADC.

Signal averaging [4], [5] is a special case of GWC with $\eta = 1$ and thus $g_1 = g_2 = g$. In the absence of thermal noise, both ADCs operate on identical input signals such that $\hat{y}_1 = \hat{y}_2$. In this case, (9) simplifies to $\bar{x}_{\text{sa}} = \hat{y}_1/g$, i.e. signal averaging does not provide any advantage over a single ADC as the quantization noise in both branches is fully correlated. If we assume that in addition to the fully correlated quantization noise, the ADCs generate uncorrelated thermal noise, we have $\hat{y}_1 \neq \hat{y}_2$ and (9) yields

$$\bar{x}_{\text{sa}} = \frac{\hat{y}_1 + \hat{y}_2}{2g}. \quad (10)$$

It can be seen that although signal averaging reduces the effective *thermal* noise in \bar{x}_{sa} by 3 dB, it cannot improve the resilience against relative power of quantization errors.

It should also be mentioned that unlike selection combining, GWC is not able to mitigate clipping errors. As soon as one of the ADCs saturates, the GWC output will be corrupted by potentially large distortions due to clipping. In the next section, we propose a hybrid scheme that benefits from the advantages of selection combining and GWC.

C. Hybrid Combining Scheme

In this section, we propose a hybrid combining scheme that overcomes the aforementioned shortcomings of selection combining and GWC. Our hybrid scheme employs GWC when both ADCs operate within their dynamic range and thus, benefits from improved resilience to quantization noise. As soon as the first ADC begins to clip the input signal, our hybrid approach switches to the selection mode and outputs

the non-clipped signal \hat{y}_2 . The operation of this scheme is described by

$$\bar{x}_{\text{hyb}} = \begin{cases} \frac{g_1 \hat{y}_1 + g_2 \hat{y}_2}{g_1^2 + g_2^2} & g_1 x \leq A \\ \frac{\hat{y}_2}{g_2} & g_1 x > A. \end{cases} \quad (11)$$

In the next section, we quantify the performance of our proposed combining schemes and compare it to that of signal averaging and selection combining. As will be demonstrated by means of computer simulations, our hybrid scheme provides resilience against both quantization and clipping noise. Therefore, we achieve an improved SNR, as well as an extended dynamic range.

VI. SIMULATION RESULTS

In this section, the performance of parallel ADC approaches is compared for the different combining methods described in Section V. A 10-bit ADC modeled according to Fig. 1 is used, with thermal noise power level -70 dB relative to the full scale of the ADC. The thermal noise of the two branches are assumed to be uncorrelated white noise. Treating the ADC and AGC as a system, the performance is measured in SNR which is calculated as the ratio between the input signal power $P(x)$ and the mean square of $e = x - \hat{x}$. Other than the thermal noise, the remaining simulation parameters are identical to those used to generate Figs. 2 and 3. The uniformly distributed signal is generated using an 8-times oversampled BPSK single carrier waveform. The Gaussian distributed signal is generated using a 512-subcarrier OFDM waveform, with BPSK modulated subcarriers. The AGC input signal x is chosen to have power $P(x) = -20$ dB. The attenuation in the second branch is set to be $\eta = 1/2$, which can be easily implemented by a passive 6 dB attenuator. The approaches compared include the selection scheme as proposed in [6] and described in Section V-A (SEL), the equal gain signal averaging scheme as proposed in [4] (Averaging), the novel gain weighted combining technique proposed in Section V-B (GWC), and the novel hybrid combiner proposed in Section V-C (HYB).

Fig. 5 shows the SNR versus AGC gain for the uniformly distributed input signal. The SNR behaviour changes when $g_1 = 14$ dB. According to Fig. 2 this is the point where the dominating contributor to the error shifts from quantization to clipping. The curve with triangle marks represents the performance of single 10bit ADC. The selection combiner [6], represented as the curve without markers, can improve the SNR in the clipping error dominated region. However it provides the worst performance in the quantization dominated range. This is because when g_1 is small, the selection combiner will only use branch 1. Hence, as shown in the figure, the selection combiner performance in this region matches that of a conventional single ADC system. The signal averaging method [4], represented as the curve with diamond markers, provides approximately 1 dB SNR improvement over the selection combiner in the quantization dominated region. This

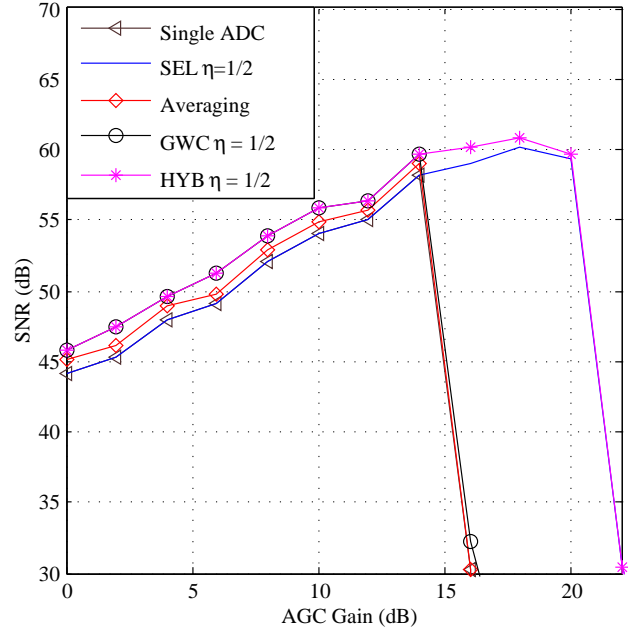


Fig. 5. Performance of parallel ADC architecture, 10-bit ADC, uniformly distributed input, BPSK modulation, thermal noise 70dB below full scale of ADC.

is achieved by reducing the impact of the thermal noise. However, the SNR of the averaging method degrades rapidly to less than 30 dB when clipping errors start to dominate as the gain is increased. The novel gain weighted combiner, marked with circle, achieves approximately 2 dB performance improvement in the quantization dominated region. This is made possible by its ability to reduce the effective quantization noise in the combined output. Similar to the averaging method, when the clipping error starts to dominate, the SNR achieved by GWC reduces rapidly. In contrast to all of the above methods, the novel hybrid combiner provides performance improvement in both the quantization error dominated region and clipping error dominated region. When $g_1 < 14$ dB, like GWC, the hybrid combiner achieves approximately 2 dB SNR improvement. When $g_1 > 14$ dB, the hybrid combiner achieves a significant SNR improvement, over 25 dB for $g_1 = 16$ dB, and also outperforms the selection method. Improvement over the selection combining method is achieved through reduction in the effective quantization error. When the gain is increased to over 20 dB, the SNR of both the selection combiner and the hybrid combiner undergo a similar drop in SNR. It can also be observed from Fig. 5, that to achieve over 55 dB SNR, the dynamic range of the ADC input is extended by 6 dB from [10 dB, 14 dB] to [10 dB, 20 dB] for both the selection combiner and the hybrid combiner. The hybrid combiner provides almost 60 dB SNR when $g_1 \in [14 \text{ dB}, 18 \text{ dB}]$, whereas the selection combiner provides 1 to 2 dB less SNR in the same region.

Fig. 6 shows the SNR versus AGC gain for the Gaussian distributed input signal. The SNR behaviour changes when

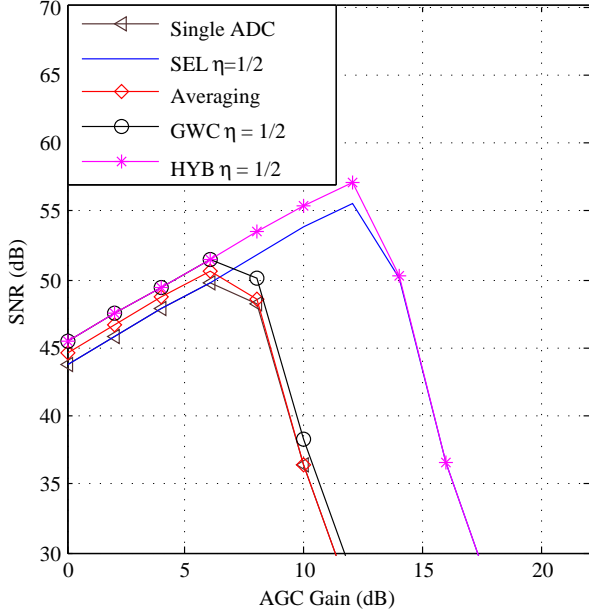


Fig. 6. Performance of parallel ADC architecture, 10-bit ADC, Gaussian distributed input, BPSK modulation, thermal noise 70dB below full scale of ADC.

$g_1 = 6$ dB. According to Fig. 3 this is the point where the dominating contributor to the error shifts from quantization to clipping. The performance of the different approaches show similar trends to those observed in Fig. 5. In the quantization dominated region, the averaging method achieves 1 dB SNR improvement against the selection combiner and conventional single ADC by reducing the effect of thermal noise, whereas the GWC and hybrid combiner achieve approximately 2 dB by reducing the effective quantization error. In the region dominated by clipping errors, the conventional single ADC, GWC and averaging method suffer significant SNR degradation. However, in this region the selection combiner and the hybrid combiner maintain the increasing SNR versus gain trend until $g_1 = 12$ dB. When the gain is increased beyond 12 dB, both the selection combiner and hybrid combiner exhibit a similar drop in SNR. It can also be observed from Fig. 6 that the ADC input dynamic range that provides over 50 dB SNR has been extended by 6 dB for the hybrid and selection combiners compared to GWC. Overall, the proposed hybrid combiner achieves approximately 2 dB SNR improvement over the selection combiner and 1 dB SNR improvement over the averaging method when $g_1 \leq 6$ dB. It also achieves a significant SNR improvement over the GWC and averaging methods, in addition to approximately 2 dB SNR improvement over the selection combiner when $6 \text{ dB} < g_1 < 14$ dB. The hybrid combiner provides a maximum SNR of 57 dB, which is 5 dB higher than that of the GWC and signal averaging, and 2 dB higher than that of the selection combiner.

VII. CONCLUSION

In this paper we have analyzed the operation of the conventional AGC and ADC front end. We have reviewed existing

approaches to using parallel ADCs and described a generalized framework in which they can be represented. We have drawn a link between this evolving field and the more mature field of multiple antenna receive diversity design. Specifically we have shown how existing schemes are analogous to equal gain combining and selection combining, while developing a new approach that is motivated by maximal ratio combining.

Based upon the generalized parallel ADC framework and analysis we have developed a novel low complexity method for *gain weighted combining* of ADC outputs. In the presence of independent thermal noise on each branch, the technique provides an SNR gain of 2 dB over a single ADC or selection combining dual ADC system as well as 1 dB gain over the averaging scheme. We have also proposed a novel *hybrid combining* approach that is able to simultaneously reduce the impact of clipping and quantization noise in the combined output, and thus increase both dynamic range and SNR. Simulation results show a 6 dB increase in dynamic range while also achieving 2 dB SNR performance gain. The proposed architecture uses an attenuator in the second ADC branch. It is expected that the value of this attenuator may be chosen to tradeoff between further increasing dynamic range at the expense of reducing the current SNR performance gain. The mechanism used to select the attenuator value and control the AGC is an interesting topic for future investigation. To apply such a technique to real system, the mismatches and misalignment of the two ADC branches and possible means to calibrate these branches need to be further investigated.

REFERENCES

- [1] J. Mitola, "Software radios—survey, critical evaluation and future directions," in *National Telesystems Conference NTC-92*, May 1992, pp. 13/15–13/23.
- [2] G. Ulbricht, "Analog-to-digital conversion – the bottleneck for software defined radio," in *Wireless Innovation Forum SDR'12-WInnComm-Europe*, Brussels, Belgium, Jun. 2012.
- [3] E. Kölbl, "Approach to solve the AGC API issue in the tactical SDR domain - a waveform provider perspective," in *Wireless Innovation Forum SDR'11-WInnComm-Europe*, Jun. 2011, pp. 48–53.
- [4] E. Seifert and A. Nauda, "Enhancing the dynamic range of analog-to-digital converters by reducing excess noise," in *IEEE Pacific Rim Conf. on Communications, Computers and Signal Processing*, Jun. 1989, pp. 574–576.
- [5] K. C. Lauritzen, S. H. Talisa, and P. Martin, "Impact of decorrelation techniques on sampling noise in radio-frequency applications," *IEEE Trans. on Instrumentation and Measurement*, vol. 59, no. 9, pp. 2272–2279, Sep. 2010.
- [6] P. M. Cruz and N. B. Carvalho, "Enhanced architecture to increase the dynamic range of SDR receivers," in *2011 IEEE Radio and Wireless Symposium (RWS)*, Jan. 2011, pp. 331–334.
- [7] W. C. Black and D. A. Hodges, "Time interleaved converter arrays," *IEEE Journal of Solid-State Circuits*, vol. SC-15, no. 6, pp. 1022–1029, Dec. 1980.
- [8] A. Goldsmith, *Wireless Communications*. Cambridge Press, 2005.
- [9] J. O. Smith III, *Mathematics of the Discrete Fourier Transform (DFT): with Audio Applications*, 2nd ed. W3K Publishing, 2007.
- [10] M. Ben-Romdhane, C. Rebai, A. Ghazel, P. Desgreys, and P. Loumeau, "Nonuniformly Controlled Analog-to-Digital Converter for SDR Multistandard Radio Receiver," *IEEE Trans. on Circuits and Systems II: Express Briefs*, pp. 862–866, 2011.
- [11] S. H. Han and J. H. Lee, "An overview of peak-to-average power ratio reduction techniques for multicarrier transmission," *IEEE Wireless Communications*, vol. 12, pp. 56–65, April 2005.